Journal of Applied Pharmaceutical Science Vol. 12(10), pp 031-048, October, 2022
Available online at http://www.japsonline.com
DOI: 10.7324/JAPS.2022.121004
ISSN 2231-3354

A triterpenoid friedelan-3β-ol isolated from *Euphorbia lactea* exhibited cytotoxic activity against HN22 cells by inducing an S-phase cell cycle arrest

Pawaris Wongprayoon[1], Sucharat Leelasart[2], Jintana Jantham[3], Yupa Pootaeng-on[4], Sittisak Oekchuae[3,5], Panupun Limpachayaporn[3], Kanok-on Rayanil[3], Purin Charoensuksai[1*]

[1]Department of Biopharmacy and Bioactives from Natural Resources Research Collaboration for Excellence in Pharmaceutical Sciences, Faculty of Pharmacy, Silpakorn University, Nakhon Pathom, Thailand.
[2]Faculty of Pharmacy, Silpakorn University, Nakhon Pathom, Thailand.
[3]Department of Chemistry, Faculty of Science, Silpakorn University, Nakhon Pathom , Thailand.
[4]Faculty of Animal Science and Agricultural Technology, Silpakorn University, Phetchaburi , Thailand.
[5]Chulabhorn Research Institute, Bangkok, Thailand.

ARTICLE INFO

Received on: 02/03/2022
Accepted on: 13/07/2022
Available Online: 04/10/2022

Key words:
Euphorbia lactea, friedelan-3β-ol, cytotoxic, anticancer, triterpenoid.

ABSTRACT

The anticancer activity of *Euphorbia lactea* Haw. (*E. lactea*) has been observed by our lab and other research groups; however, the identity of the bioactive compounds harboring the anticancer effect remains unknown. Here, we report the first isolation of four triterpenoidal compounds, i.e., friedelin [**1**], friedelan-3β-ol [**2**], taraxerol [**3**], and friedelan-3α-ol [**4**], from the n-hexane fraction of the *E. lactea* extract. The cytotoxic activities of these compounds were investigated in several cancer cell lines, including HN22, HepG2, HCT116, and HeLa. These compounds exhibited a dose-dependent cytotoxic activity against HN22, HepG2, and HCT116, while the marginal cytotoxic effect was observed in HeLa cells. Among the four bioactive compounds, compound **2** exhibited the most prominent anticancer effect against HN22 cells. Flow cytometry analysis of HN22 cells treated with the compound revealed that compound **2** induced a cell cycle arrest at the S-phase, while apoptosis was not induced at the same concentration and exposure time. In summary, our results highlighted *E. lactea* as an attractive candidate for anticancer research and identified compound **2** as a chemical constituent of *E. lactea* harboring anticancer activity.

INTRODUCTION

Cancer is a disease caused by the accumulation of genetic defects within human cells, which culminates in an uncontrolled proliferative state. Current therapy for cancers includes radiation, surgical removal, and pharmacological treatments with various anticancer agents. Rigorous research in the discovery and development of anticancer agents has led to the establishment of many anticancer agents ranging from conventional chemotherapeutic agents to targeted therapy using small-molecule drugs and monoclonal antibodies. However, despite the availability of a vast collection of effective anticancer agents, the acquisition of a drug-resistant phenotype (Holohan *et al*., 2013; Housman *et al*., 2014) and serious adverse reactions associated with certain chemical entities still limit the outcome of anticancer pharmacotherapy. Thus, the development of novel anticancer compounds which will add to the variety of treatment options is likely to confer benefits to cancer patients.

Although the pathogenesis of cancers is widely accepted to be heterogenic in nature, driven by an astounding repertoire

**Corresponding Author*
Purin Charoensuksai, Department of Biopharmacy and Bioactives from Natural Resources Research Collaboration for Excellence in Pharmaceutical Sciences, Faculty of Pharmacy, Silpakorn University, Nakhon Pathom, Thailand.
E-mail: charoensuksai_p @ su.ac.th

of genetic and epigenetic defects, the deregulation of cell cycle progression and programmed cell death pathways holds a central place in cancer pathogenesis (Evan and Vousden, 2001). Many anticancer agents used clinically and in clinical trials have been shown to directly or indirectly affect cell cycle progression or apoptosis in cancer cells (Sun *et al*., 2021; Wong, 2011). Therefore, the assessment of the activity of putative anticancer compounds in the interference with cell cycle progression or apoptosis in cancer cells should serve as an additional test to verify cytotoxicity and reveal the anticancer potential of novel therapeutic entities.

Euphorbiaceae is a large botanical family encompassing over 2,000 species of unique flora with distinctive milky latex and flower shape. The medicinal property of *Euphorbia* has been documented in both traditional medicinal records and contemporary pharmaceutical research. There are over 100 publications documenting the cytotoxic activity of extracts and pure compounds isolated from over 60 species of *Euphorbia* (Wongrakpanich and Charoensuksai, 2018). Phytochemical research of *Euphorbia* has led to the isolation of over 500 compounds, especially terpenoids (Shi *et al*., 2008). Many of these compounds have been shown to exert anticancer activity through the induction of apoptosis (Wongrakpanich and Charoensuksai, 2018).

Endemic to tropical regions of the world and abundantly found in Thailand, *Euphorbia lactea* Haw. (*E. lactea*) is a succulent plant with a distinctive triangular stem. Despite the documented anticancer properties of other *Euphorbia* species, only a few publications have shed light on the anticancer activities of *E. lactea*. First, El-Manawaty *et al*. (2013) reported that the methanolic extracts of *E. lactea* exhibited cytotoxic activity against hepatocellular carcinoma cell line HepG2 and colorectal cancer cell line HCT116. This observation was further echoed by a report from another group describing the cytotoxic effects of the *E. lactea* crude methanolic extract in HepG2 and breast cancer cell line MCF7 (El-Hawary *et al*., 2020). Our lab previously reported the inhibitory effect of the crude ethanolic extract of *E. lactea* against the viability and migration of HN22 cancer cells (Wongprayoon and Charoensuksai, 2018). Taken together, the anticancer activity of the *E. lactea* extract has been documented through several independent reports; nevertheless, the chemical entities responsible for the anticancer activity of *E. lactea* are yet to be identified.

MATERIALS AND METHODS

Plant materials

The *E. lactea* specimen used in this experiment was propagated from cuttings collected from a mother plant and cultivated in our greenhouse in Bangkok, Thailand. Plant collection was carried out in May 2019. The species identification was made by a comparison of morphologies between the specimen and pictures of *E. lactea* in plant databases such as http://www.eol.org and https://www.cabi.org. A voucher specimen (SUPY. PC1) was deposited at the Herbarium of the Faculty of Pharmacy, Silpakorn University, Thailand.

Chemicals and reagents

The common solvents, including ethanol, n-hexane, ethyl acetate (EtOAc), and n-butanol (n-BuOH), for extraction and chromatography were purchased from Merck (Germany). Deuterated chloroform ($CDCl_3$, 99.98% D) for nuclear magnetic resonance (NMR) analysis and cerium (IV) sulfate were purchased from Sigma-Aldrich (St. Louis, MO). Column chromatography was carried out on silica gel (230–400 mesh, Merck). Aluminum sheets of silica gel (60 F254, Merck) were used for thin-layer chromatography (TLC).

Head-and-neck cancer cell line HN22, hepatocellular carcinoma cell line HepG2, colorectal cancer cell line HCT119, and cervical cancer cell line HeLa were kindly provided by Prof. Praneet Opanasopit, Faculty of Pharmacy, Silpakorn University, Thailand. Immortalized human keratinocyte cell line HaCaT was given by Assist. Prof. Dr. Veerawat Teeranachaidekul, Department of Pharmacy, Faculty of Pharmacy, Mahidol University, Thailand. Dulbecco's modified Eagle's medium (DMEM), minimum essential media (MEM), fetal bovine serum (FBS), nonessential amino acids, GlutaMAX, and penicillin/streptomycin solution were purchased from Gibco (Waltham, MA)

Dimethyl sulfoxide (DMSO), Triton-X 100, and 3-(4,5-dimethylthiazol-2-yl)-2,5-diphenyltetrazoliumbromide (MTT) were purchased from Sigma-Aldrich. Hydroxypropyl-β-cyclodextrin (CAVASOL W7 HP Pharma) from Wacker Chemie AG (Munich, Germany) was given by Prof. Praneet Opanasopit. Irinotecan (Irinotel) was purchased from Fresenius Kabi Oncology, India. DNase-free RNase A was purchased from Bio Basic (Amherst, NY). Propidium iodide was purchased from Life Technologies (Carlsbad, CA). FITC-conjugated annexin-V A13199 was purchased from Thermo Fischer (Waltham, MA).

Extraction and isolation

The aerial parts of *E. lactea* were cut into thin slices and left to air-dry in a parabola dome solar drying chamber for 5 days. The dried specimens (2.68 kg) were crushed and extracted with 95% ethanol at room temperature (7 l × 3 times). The extract was concentrated under reduced pressure to give a dark brown residue (613.40 g). The residue was resuspended in water (2 l) and then extracted with n-hexane, EtOAc, and n-BuOH (each solvent 1,400 ml × 3), successively. The respective solvents were evaporated to dryness at 40°C under reduced pressure to yield the n-hexane (94.02 g), EtOAc (33.11 g), and n-BuOH (36.82 g) fractions. The remaining aqueous phase was concentrated to give the H_2O fraction (428.46 g). A portion of the n-hexane fraction (46.15 g) was subjected to flash column chromatography over silica gel and eluted with n-hexane-EtOAc (gradient from 100% n-hexane to 100% EtOAc) to afford 16 fractions (H_1–H_{16}). Fraction H_6 (0.6030 g) was recrystallized from ethanol to give **1** (0.1069 g). Fraction H_8 (0.3297 g) was further subjected to a silica gel column, eluted with n-hexane–EtOAc (99:1–97:3) to yield **2** (0.2006 g). Fraction H_{12} (0.5303 g) was recrystallized from ethanol to give **3** (0.1879 g). Further purification of fraction H_{16} (0.5584 g) by column chromatography over a silica gel, using n-hexane–EtOAc (99:1–95:5), afforded **4** (0.1534 g).

Structural identification

The chemical structures of pure compounds **1**–**4** were determined by mass spectrometry and NMR spectroscopy. High-resolution electrospray ionization mass spectrometry (HRESIMS) experiments were performed on a Micro TOF Brüker Daltonics mass spectrometer. The ^{1}H and ^{13}C-NMR data were recorded at 300 MHz and 75 MHz on a Brüker AVANCE 300 NMR spectrometer using tetramethylsilane as an internal reference.

Column chromatography was carried out using silica gel (230–400 mesh, Merck). TLC was performed, and spots were detected under ultraviolet light at 254 nm or by spraying with a solution of 1% cerium(IV) sulfate in 10% H_2SO_4 followed by heating.

By comparison of ^{1}H-NMR, ^{13}C-NMR, and mass spectral data of each compound (Supplementary Figs. S1–S12) with those reported in the literature, the isolated compounds were identified as pentacyclic triterpenoids including friedelin [**1**], friedelan-3β-ol [**2**], taraxerol [**3**], and friedelan-3α-ol [**4**]. Physical and spectroscopic data of these compounds are shown as follows.

Friedelin [**1**] was obtained as white crystals with melting point 254°C–258°C; ^{1}H-NMR (Supplementary Fig. S1) (300 MHz, $CDCl_3$) δ ppm: 2.40 (1H, m, H-6b), 2.25 (1H, q, J = 6.3 Hz, H-4), 1.97 (1H, m, H-1b), 1.75 (1H, m, H-6a), 1.69 (1H, m, H-1b), 1.18 (3H, s, H-28), 1.05 (3H, s, H-27), 1.01 (3H, s, H-26), 1.00 (3H, s, H-30), 0.95 (3H, s, H-29), 0.89 (3H, d, J = 6.3 Hz, H-23), 0.87 (3H, s, H-25), and 0.73 (3H, s, H-24); ^{13}C-NMR (Supplementary Fig. S2) (75 MHz, $CDCl_3$) δ ppm: 213.3 (C-3), 59.5 (C-10), 58.2 (C-4), 53.1 (C-8), 42.8 (C-18), 42.1 (C-5), 41.5, (C-2), 41.3 (C-6), 39.7 (C-13), 39.3 (C-22), 38.3 (C-14), 37.4 (C-9), 36.0 (C-16), 35.6 (C-11), 35.3 (C-19), 35.0 (C-29), 32.8 (C-21), 32.4 (C-15), 32.1 (C-28), 31.8 (C-30), 30.5 (C-12), 30.0 (C-17), 28.2 (C-20), 22.3, (C-1), 20.3 (C-26), 18.7 (C-27), 18.2 (C-7), 17.9 (C-25), 14.7 (C-24), and 6.8 (C-23); HRESIMS (Supplementary Fig. S9) *m/z* 449.3757 $[M+Na]^+$ (calculated mass for $C_{30}H_{50}ONa$, 449.3760).

Friedelan-3β-ol [**2**] was obtained as white amorphous powder with melting point 274°C–280°C; ^{1}H-NMR (Supplementary Fig. S3) (300 MHz, $CDCl_3$) δ ppm: 3.73, (1H, m, H-3), 1.90 (1H, m, H-2b), 1.73 (1H, dt, J = 9.6, 3.3 Hz, H-6b), 1.22 (1H, m, H-2a), 1.17 (3H, s, H-28), 1.01 (3H, s, H-27), 1.00 (3H, s, H-30), 0.99 (3H, s, H-26), 0.98 (1H, m, H-6a) 0.96 (3H, s, H-24), 0.95 (3H, s, H-29), 0.93 (3H, d, J = 6.0 Hz, H-23), and 0.86 (3H, s, H-25); ^{13}C-NMR (Supplementary Fig. S4) (75 MHz, $CDCl_3$) δ ppm: 72.8 (C-3), 61.3 (C-10), 53.2 (C-8), 49.2 (C-4), 42.8 (C-18), 41.7 (C-6), 39.7 (C-14), 39.3, (C-22), 38.4 (C-13), 37.8 (C-5), 37.1 (C-9), 36.1 (C-16), 35.6 (C-11), 35.3 (C-19), 35.2 (C-2), 35.0 (C-29), 32.8 (C-21), 32.3 (C-15), 32.1 (C-28), 31.8 (C-30), 30.6 (C-12), 30.0 (C-17), 28.2 (C-20), 20.1 (C-26), 18.7 (C-27), 18.3 (C-25), 17.6, (C-7), 16.4 (C-24), 15.8 (C-1), and 11.6 (C-23); HRESIMS (Supplementary Fig. S10) *m/z* $[M+NH_4]^+$ 446.4342 (calculated mass for $C_{30}H_{52}O+NH_4^+$, 446.4356).

Taraxerol [**3**] was obtained as white crystals with melting point 269°C–272°C; ^{1}H-NMR (Supplementary Fig. S5) (300 MHz, $CDCl_3$) δ ppm: 5.53 (1H, dd, H-15, J = 8.2, 3.2 Hz), 3.19 (1H, m, H-3), 2.03 (1H, dt, J = 12.5, 3.2 Hz, H-7b), 1.96 (1H, dd, J = 14.7, 3.1 Hz, H-16b), 1.63 (1H, m, H-16a), 1.34 (1H, m, H-7a), 1.09 (3H, s, H-26), 0.98 (3H, s, H-23), 0.95 (3H, s, H-29), 0.93 (3H, s, H-25), 0.90 (6H, s, H-27, H-30), 0.82 (3H, s, H-28), and 0.80 (3H, s, H-24); ^{13}C-NMR (Supplementary Fig. S6) (75 MHz, $CDCl_3$) δ ppm: 158.1 (C-14), 116.9 (C-15), 79.1 (C-3), 55.5 (C-5), 49.3 (C-9), 48.7 (C-18), 41.3 (C-7), 39.0 (C-8), 38.8 (C-4), 38.0 (C-10), 37.7 (C-1, C-16), 37.6 (C-13), 36.7 (C-16), 35.8 (C-17), 35.1 (C-22), 33.7 (C-21), 33.4 (C-29), 33.1 (C-12), 29.9 (C-30), 29.8 (C-28), 28.8 (C-20), 28.0 (C-23), 27.1 (C-2), 25.9 (C-26), 21.3 (C-27), 18.8 (C-6), 17.5 (C-11), 15.5 (C-24), and 15.4 (C-25); HRESIMS (Supplementary Fig. S11) *m/z* 449.3768 $[M+Na]^+$ (calculated mass for $C_{30}H_{50}ONa$, 449.3760).

Friedelan-3α-ol [**4**] was obtained as white amorphous powder with melting point 294°C–298°C; ^{1}H-NMR (Supplementary Fig. S7) (300 MHz, $CDCl_3$) δ ppm: 3.35, (1H, m, H-3), 2.06 (1H, m, H-2b), 1.77 (1H, dt, J = 12.8, 3.2 Hz, H-6b), 1.22 (1H, m, H-2a), 1.17 (3H, s, H-28), 1.03 (1H, m, H-6a), 1.01 (3H, s, H-27), 0.99 (3H, s, H-30), 0.99 (3H, s, H-26), 0.94 (3H, s, H-29), 0.89 (3H, d, J = 6.6 Hz, H-23), 0.81 (3H, s, H-25), and 0.77 (3H, s, H-24); ^{13}C-NMR (Supplementary Fig. S8) (75 MHz, $CDCl_3$) δ ppm: 72.2 (C-3), 60.1 (C-10), 53.2 (C-4), 53.0 (C-8), 42.8 (C-18), 41.4 (C-6), 39.7 (C-14), 39.3, (C-22), 38.3 (C-13), 38.1 (C-5), 37.0 (C-9), 36.7 (C-2), 36.1 (C-16), 35.5 (C-11), 35.3 (C-19), 35.0 (C-29), 32.8 (C-21), 32.4 (C-15), 32.1 (C-28), 31.8 (C-30), 30.6 (C-12), 30.0 (C-17), 28.2 (C-20), 20.2 (C-26), 19.6 (C-1), 18.7 (C-27), 18.1 (C-25), 17.8 (C-7), 14.6 (C-24), and 9.9 (C-23); HRESIMS (Supplementary Fig. S12) *m/z* 451.3855 $[M+Na]^+$ (calculated mass for $C_{30}H_{52}ONa$, 451.3916).

Cell culture

HN22, HepG2, and HCT116 were maintained in DMEM supplemented with 10% FBS and 1% GlutaMAX. HeLa was maintained in MEM supplemented with 10% FBS, 1% nonessential amino acids, and 1% GlutaMAX. HaCaT was maintained in DMEM supplemented with 10% FBS. All culture media contained 100 units/mL penicillin and 100 µg/mL streptomycin. Cells were cultured in a humidified atmosphere containing 5% CO_2 and temperature-controlled at 37°C.

Determination of cell viability by MTT assay

The crude extract (n-hexane, EtOAc, and n-BuOH) and H_2O fractions were dissolved in DMSO. The pure compounds **1–4** were dissolved in a mixture solution of DMSO containing 30% w/v hydroxypropyl-β-cyclodextrin (DMSO-HPBCD).

Cell viability determination by the MTT assay was performed following an established protocol (Kumar *et al*., 2018) with some modifications. Briefly, 8,000 cells were seeded into each well of a 96-well plate and allowed to attach overnight. Due to the limited solubility of the extract, fractions, and pure compounds in the dissolving vehicle, the maximal concentrations investigated were 500 µg/ml for extracts and fractions and 110 µM for pure compounds. Cells were then incubated with varying concentrations of the extracts (500–1.953 µg/ml final concentration) or pure compounds (110–0.176 µM) for 72 hours. 100 µM irinotecan was used as a positive control. The vehicles used to dissolve the test agents, i.e., DMSO for plant extract and fractions or DMSO-HPBCD for **1–4**, were used as negative controls. The final concentration of DMSO and DMSO-HPBCD was maintained at 0.5% w/v for all test conditions. Afterward, 25 µl of 5 mg/ml MTT dissolved in phosphate buffer saline (PBS) was added to each well and incubated for 4 hours. Culture media were then discarded, and 100 µl of DMSO was added to each well to dissolve formazan crystals. Absorbance at 550 nm was measured using a microplate reader (Model No. AOPUS01 and A153601; Packard BioScience Company, CT). All experiments were performed in triplicate.

Cell cycle analysis by flow cytometry

The analysis of cell cycle distribution by propidium iodide staining and flow cytometry was performed according to an established protocol (Crowley *et al*., 2016a) with some modifications. Briefly, HN22 cells were cultured in the presence of 110 µM of **2** or vehicle control for 72 hours. Cells were then washed with PBS, harvested, and fixed with 70% ice-cold ethanol. Afterward, cells were washed twice with ice-cold PBS and treated

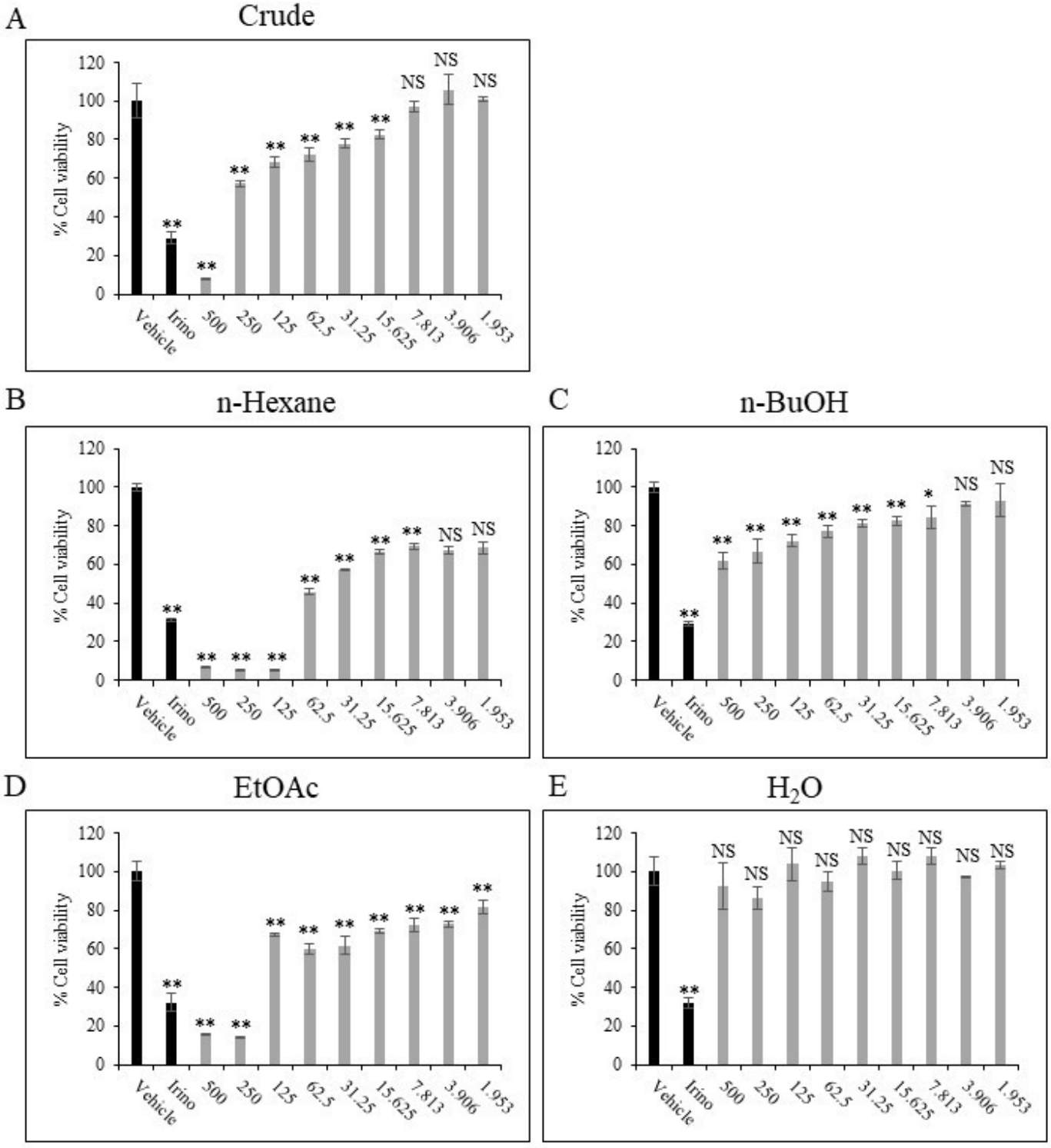

Figure 1. Cytotoxic activity of *E. lactea* extracts toward HN22 cells. HN22 cells were treated with DMSO (vehicle control), 100 μM irinotecan, or extracts at concentrations ranging from 500 to 1.953 μg/ml for 72 hours as described Materials and Methods in the section. ** $p < 0.01$, * $p < 0.05$, NS $p \geq 0.05$ compared to vehicle control.

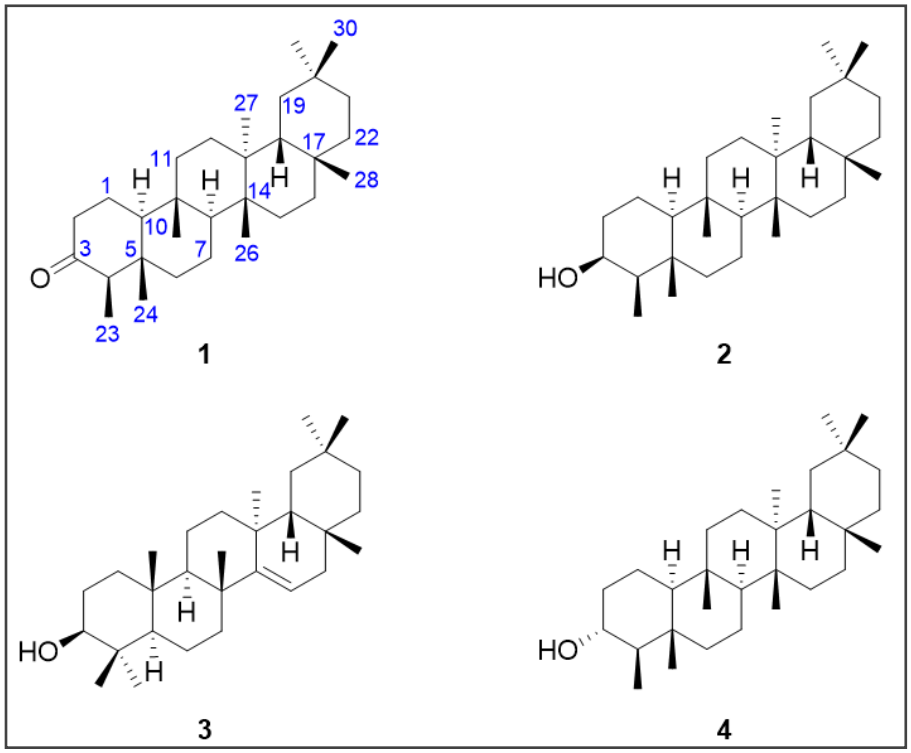

Figure 2. Chemical structures of friedelin [**1**], friedelan-3β-ol [**2**], taraxerol [**3**], and friedelan-3α-ol [**4**] isolated from the n-hexane fraction of *E. lactea.*

with 100 µg/mL of DNase-free RNase A in PBS containing 0.1% v/v Triton-X 100 for 5 minutes at room temperature. Cells were then stained with 20 µg/ml propidium iodide in PBS containing 0.1% v/v Triton-X 100 for 15 minutes at room temperature in the dark. Cell cycle distribution profiles were obtained with a flow cytometer (Attune NxT, Thermo Fischer). Data were analyzed with Attune NxT Software (Thermo Fischer). All experiments were carried out in triplicate.

Analysis of apoptotic cells by flow cytometry

The flow cytometry analysis of cells undergoing apoptosis by annexin-V and propidium iodide double staining was carried out following an established protocol (Crowley *et al*., 2016b) with some modifications. Briefly, HN22 cells were cultured in the presence of 110 µM of **2**, 20 µM Irinotecan for positive control, or vehicle for negative control for 72 hours. Cells were then collected, resuspended in PBS, and counted. For each condition, 1×10^5 cells were collected to stain with 5 µl of FITC-conjugated annexin-V in binding buffer (0.1 M HEPES, 1.5 M NaCl, 50 mM $MgCl_2$, 50 mM KCl, and 18 mM $CaCl_2$, pH 7.4) for 15 minutes at room temperature while protected from light. Afterward, propidium iodide was added to a final concentration of 5 µg/ml and incubated for 15 minutes at room temperature while protected from light. Then, the cells were analyzed by a flow cytometer (Attune NxT, Thermo Fischer). Data were analyzed with Attune NxT Software (Thermo Fischer).

Statistical analysis

One-way analysis of variance with Tukey's HSD *post-hoc* test was used to analyze the statistical significance of cell viability experiments of the extract, fractions, and pure compounds. Student's *t*-test test was used for cell cycle experiments. The software GraphPad Prism version 7 (GraphPad Software Inc., La Jolla, CA) was used for statistical analysis. $p < 0.05$ was considered statistically significant.

RESULTS AND DISCUSSION

Our group previously reported the cytotoxic activity of the crude hydroalcoholic extract of fresh *E. lactea* against HN22 cells (Wongprayoon and Charoensuksai, 2018). This prompted us to ask whether *E. lactea* contains lead compound(s) with potent anticancer activity. First, we sought to study the cytotoxic activity of the crude extract collected from the extraction of dried and ground *E. lactea* with 95% ethanol. Indeed, the crude extract of *E. lactea* exhibited a dose-dependent cytotoxic activity against HN22 cells with statistical significance in all concentrations from 15.625 µg/ml and above (Fig. 1A). Next, we sought to further investigate the cytotoxic effect by sequentially partitioning the crude extract with n-hexane, EtOAc, and n-BuOH to collect refined extracts with different polarities. The cytotoxic effect of n-hexane, EtOAc, n-BuOH, and the H_2O fractions was then studied using the same concentration interval of the crude extract. The result revealed that the cytotoxic activity was markedly increased in the n-hexane and EtOAc fractions, while such effect was diminished in the n-BuOH and negligible in the H_2O fraction (Fig. 1).

As the n-hexane fraction exhibited the most potent cytotoxic effect, this fraction was subjected to further purification to obtain pure chemical entities. Purification of the n-hexane fraction by chromatography techniques resulted in the isolation

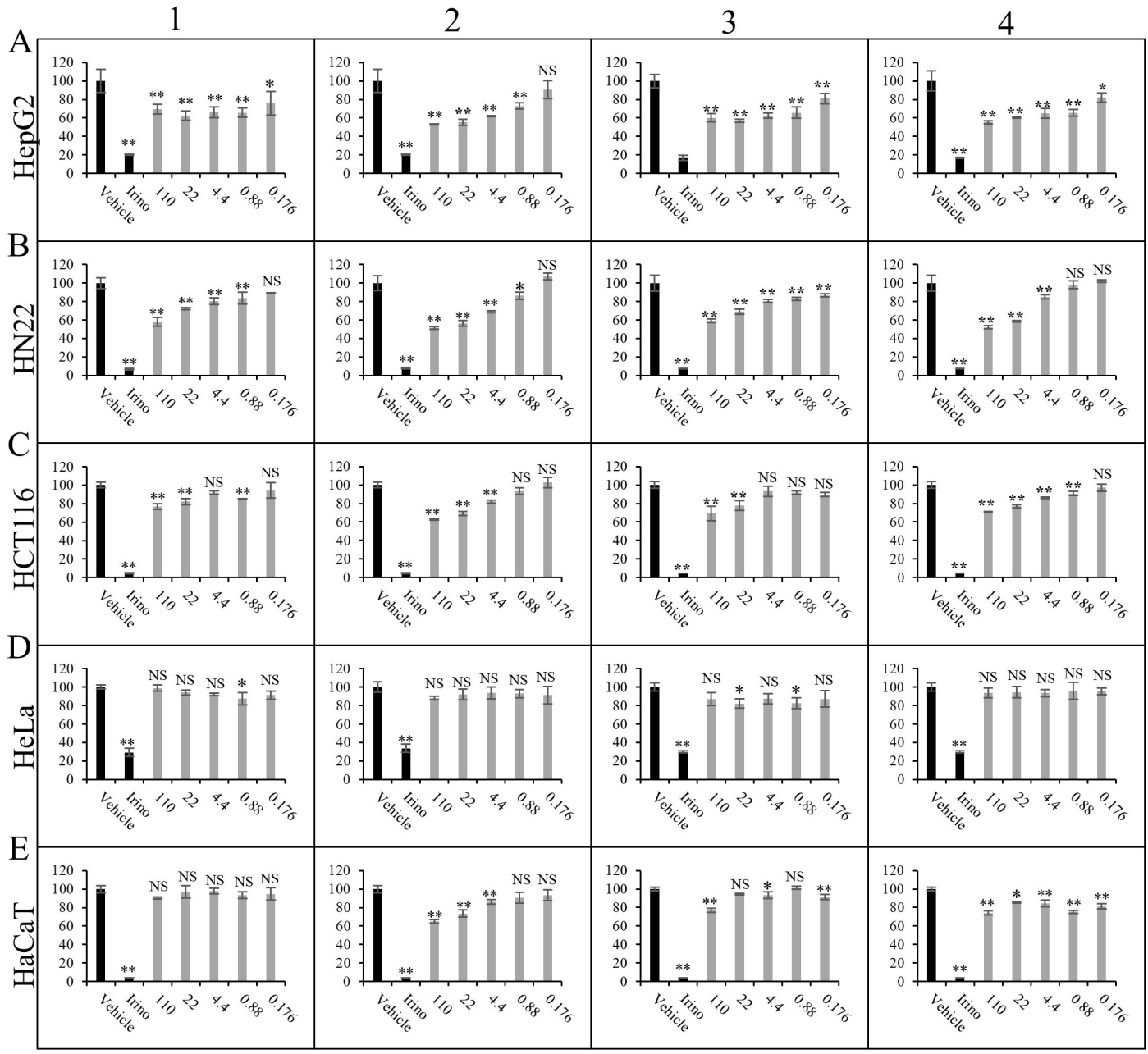

Figure 3. Cytotoxic activity of **1–4** toward cancer cell lines. (A) HepG2, (B) HN22, (C) HCT116, (D) HeLa, and (E) immortalized human keratinocyte cell line HaCaT were treated with vehicle control, 100 µM irinotecan, or **1–4** at concentrations ranging from 110 to 0.176 µM for 72 hours as described in the Materials and Methods section. ** $p < 0.01$, * $p < 0.05$, NS $p \geq 0.05$ compared to vehicle control.

of four triterpenoids as the major constituents. The triterpenoids were identified as friedelin [**1**], friedelan-3β-ol [**2**], taraxerol [**3**], and friedelan-3α-ol [**4**] (Fig. 2). The chemical structures of all compounds were elucidated based on their 1D and 2D NMR spectroscopic data and by comparison of their physical and spectroscopic data with literature reports (Govindachari *et al*., 1967; Jamal *et al*., 2009; Koay *et al*., 2013; Ndwigah *et al*., 2013). In addition, the molecular mass of all isolated compounds agreed with the measured m/z analyzed by HRESIMS. The isolation of these compounds has been reported in other *Euphorbia* species. For example, **1** was previously isolated from *Euphorbia tortilis* (Anju *et al*., 2018) and *Euphorbia geniculata* (Farozi *et al*., 2015). **2** was previously detected in *E. neriifolia* (Anjeneyulu *et al*., 1973) and *Euphorbia antiquorum* (Min *et al*., 1989). **3** was previously purified from *E. antiquorum* (Min *et al*., 1989), *Euphorbia myrsinites* (Aynehchi *et al*., 1972), and *E. neriifolia* (Anjeneyulu *et al*., 1973). **4** was previously isolated from *E. neriifolia* (Anjeneyulu *et al*., 1973). However, to our knowledge, our report describes the first detection and isolation of these compounds from the species *E. lactea*. These compounds share a core pentacyclic triterpenoid structure, which has been shown to have various pharmacological effects, including anticancer activity (Ghante and Jamkhande, 2019).

Cytotoxic activities of the isolated compounds **1**–**4** were then investigated in four cancer cell lines, namely HepG2, HN22, HCT116, and HeLa, while HaCaT was used as a representative noncancerous cell line (Fig. 3). Compounds **1**–**4** exhibited a dose-dependent cytotoxic effect on HepG2, HN22, and HCT116 with more effect on cancer cells than untransformed cells. Among the four compounds, **2** appeared to be the most potent, with the strongest inhibition effect on HN22 and HepG2 cells. Interestingly, all compounds exhibited marginal or no effect on HeLa cells, suggesting that the cytotoxic effect of these triterpenoids is likely dependent on cell type.

Given that **2** exhibited the most prominent cytotoxic effect, we then sought to further explore the underlying molecular mechanism likely associated with such activity, i.e., the induction of cell cycle arrest and apoptosis. First, the effect of **2** on the cell cycle distribution of HN22 and HepG2 cells was studied. No change in cell cycle distribution was detected in HepG2 cells treated with **2** (Fig. 4A and B). However, treatment of HN22 cells with **2** is accompanied by a statistically significant increase in cells at the S-phase, indicative of the induction of an S-phase cell cycle arrest (Fig. 4C and D). Next, an apoptosis assay by flow cytometry analysis of cells stained with propidium iodide and FITC-conjugated annexin-V was performed on HN22 cells treated with **2**. While apoptotic cells were markedly increased upon treatment with the positive control irinotecan (Fig. 5), the percentage of early and late apoptotic cells remained unchanged upon treatment with **2**, suggesting that the cytotoxic activity of **2** toward HN22 cells was not mediated through apoptosis, at least at the concentration and exposure time we investigated.

Indeed, the cytotoxic activity of **2** has previously been tested against several cancer cell lines. While it generally exhibited mild cytotoxic activity against many cancer cell lines (Monkodkaew *et al*., 2009; Oliveira *et al*., 2012; Su *et al*., 2009), **2** markedly suppressed the viability of certain types of cancer. First, Martucciello *et al*. (2010) reported that **2** inhibited the cell viability of the Kaposi sarcoma cell line by ~30% at 20 µM. Later, Yessoufou *et al*. (2015) reported that, among the five cancer types tested, including HeLa, MCF7, Jurkat, HT-29, and T24, **2** exhibited the strongest cytotoxic activity against the T24 bladder cancer cell line with an IC_{50} of 15.61 µg/mL (~35 µM). In line with this observation, we detected >40% reduction in cell viability in HN22 and HepG2 cells treated with **2** at 22 µM, suggesting that

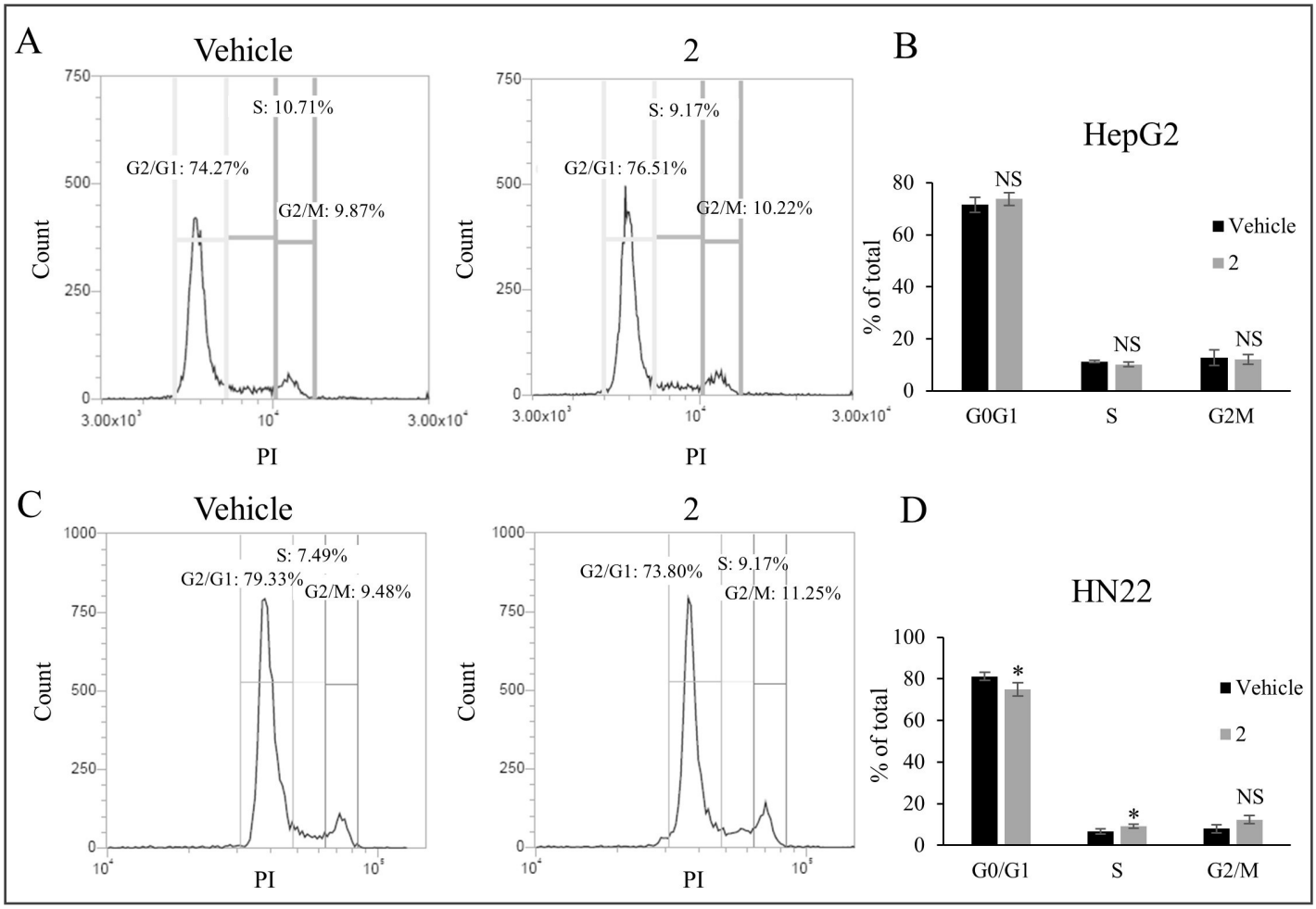

Figure 4. Cell cycle distribution analysis of cancer cell lines treated with **2**. (A) Histogram showing cell cycle distribution of HepG2 cells treated with 110 µM of **2** or vehicle control. (B) Quantitation of HepG2 cells treated with 110 µM of **2** or vehicle control in the G0/G1, S, and G2/M phases of the cell cycle. (C) Histogram showing cell cycle distribution of HN22 cells treated with 110 µM of **2** or vehicle control. (D) Quantitation of HN22 cells treated with 110 µM of **2** or vehicle control in the G0/G1, S, and G2/M phases of the cell cycle. * $p < 0.05$, NS $p \geq 0.05$ compared to vehicle control.

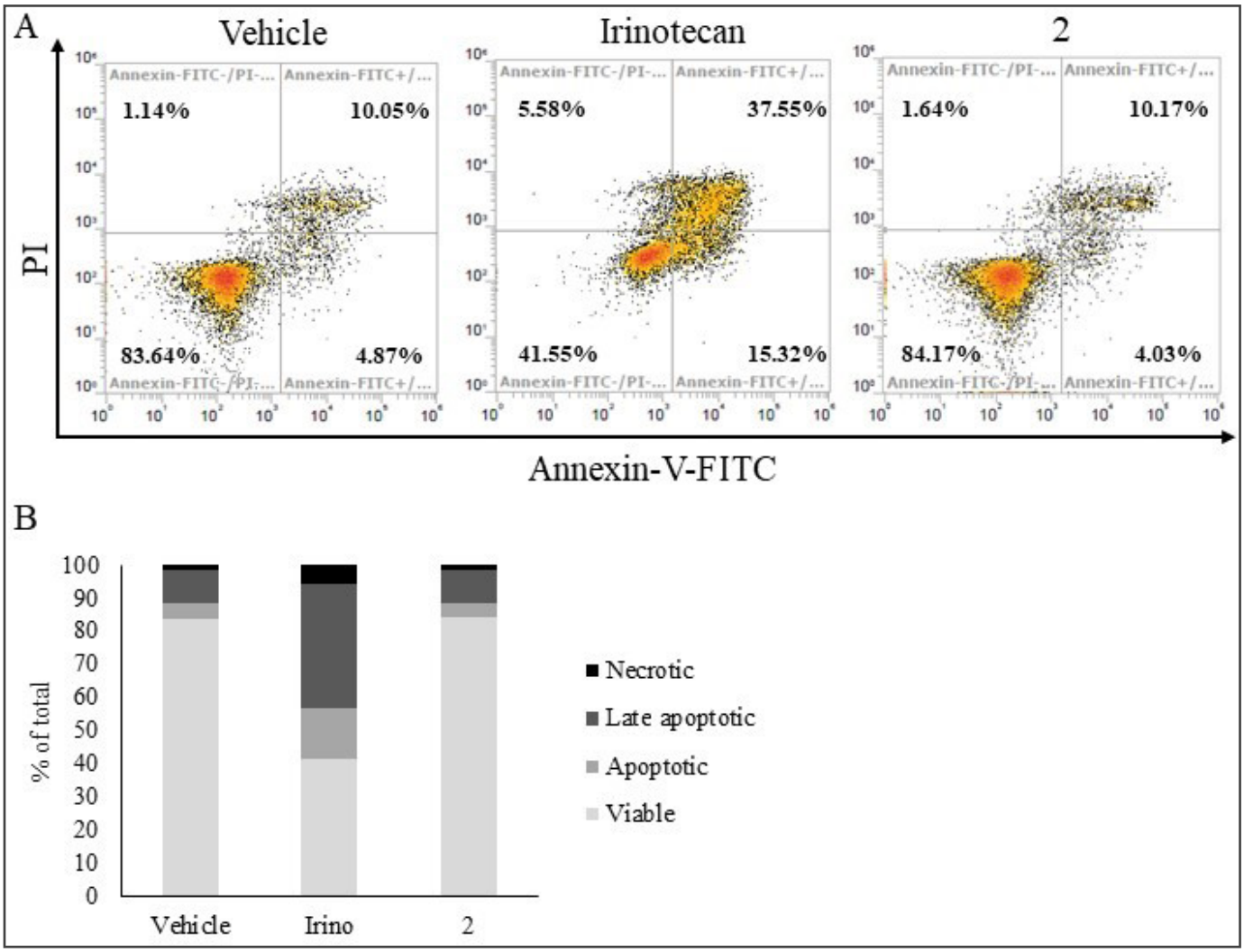

Figure 5. Analysis of apoptotic cells by flow cytometry. (A) Density plot of HN22 cells treated with vehicle control, 20 µM irinotecan (positive control), and 110 µM of **2** at 72 hours. (B) Quantitation of viable, apoptotic, late apoptotic, and necrotic cells as shown in (A).

the cytotoxic activity of **2** may be more robust toward these types of cancer. Indeed, these observations need to be confirmed in a controlled test. Moreover, the molecular mechanism underlying the anticancer activity of **2** was largely unexplored. Previous reports utilizing molecular docking analysis suggested that **2** may be able to interact with DNA methyltransferase 1 (Wilaputraka *et al*., 2017) and HER2 and EGFR (Perumal *et al*., 2016). Our result thus shed some light on the mechanism of action of **2** in that its anticancer effect was mediated through interference with the cell cycle, particularly a cell cycle arrest at the S-phase, and not through the induction of apoptosis like many anticancer compounds (Pistritto *et al*., 2016). Therefore, it is of particular interest to study the effect of **2** when used in combination with other anticancer agents in susceptible cancer types.

CONCLUSION

This work reported the first isolation of four triterpenoidal compounds, namely friedelin [**1**], friedelan-3β-ol [**2**], taraxerol [**3**], and friedelan-3α-ol [**4**], from the n-hexane fraction of *E. lactea.* Cytotoxic activity of these compounds was observed in the HN22, HepG2, and HCT116 cell lines. Among the four compounds, **2** exhibited a prominent anticancer effect against HN22 cells. Subsequent analysis of cell cycle distribution and cells undergoing apoptosis using flow cytometry revealed that treatment with **2** was associated with an increase in cells at the S-phase in HN22 while apoptosis was unperturbed. In summary, our results highlighted *E. lactea* as a plant with anticancer activity and identified **2** as a chemical constituent harboring anticancer activity in *E. lactea.*

ACKNOWLEDGMENTS

The authors thank the Faculty of Pharmacy, Silpakorn University, for research facilities and instruments. They also thank Prof. Serm Janjai for his assistance in the dehydration of the plant specimen by using the parabola dome solar drying chamber. The authors thank Prof. Praneet Opanasopit for providing the cell lines and reagents. They also thank Asst. Prof. Dr. Nattiya Kapol for the irinotecan.

FUNDING

This publication is a part of research project "The development of natural products for the treatment of age-related diseases" (SURIC 62/01/43) funded by the National Research

Council of Thailand through Silpakorn University Research, Innovation and Creativity Administration Office (SURIC).

AUTHOR CONTRIBUTIONS

All authors made substantial contributions to conception and design, acquisition of data, or analysis and interpretation of data; took part in drafting the article or revising it critically for important intellectual content; agreed to submit to the current journal; gave final approval of the version to be published; and agree to be accountable for all aspects of the work. All the authors are eligible to be an author as per the international committee of medical journal editors (ICMJE) requirements/guidelines.

CONFLICTS OF INTEREST

The authors report no financial or any other conflicts of interest in this work.

ETHICAL APPROVALS

This study does not involve experiments on animals or human subjects.

DATA AVAILABILITY

All data generated and analyzed are included within this research article.

PUBLISHER'S NOTE

This journal remains neutral with regard to jurisdictional claims in published institutional affiliation.

ABBREVIATIONS

n-BuOH:	n-Butanol
DMEM:	Dulbecco's modified Eagle's medium
DMSO :	Dimethyl sulfoxide
DMSO-HPBCD:	30% w/v hydroxypropyl-β-cyclodextrin in DMSO
EtOAc:	Ethyl acetate
E. lactea:	*Euphorbia lactea* Haw.
FBS:	Fetal bovine serum
HPBCD:	Hydroxypropyl-β-cyclodextrin
HRESIMS:	High-resolution electrospray ionization mass spectrometry
MEM:	Minimum essential media
MTT:	3-(4,5-Dimethylthiazol-2-yl)-2,5-diphenyltetrazoliumbromide
NMR:	Nuclear magnetic resonance
PBS:	Phosphate buffer saline.

REFERENCES

Anjeneyulu ASR, Row LR, Subrahmanyam C, Murty KS. Crystalline constituents from euphorbiaceae-XIII. The structure of a new triterpene from *Euphorbia nerifolia* L. Tetrahedron, 1973; 29(23):3909–14.

Anju V, Singh A, Shilpa G, Kumar B, Priya S, Sabulal B, Rameshkumar KB. Terpenes and biological activities of *Euphorbia tortilis*. Lett Org Chem, 2018; 15(3):221–5.

Aynehchi Y, Mojtabaii M, Yazdizadeh K. Chemical examination of *Euphorbia myrsinitis* linn. J Pharm Sci, 1972; 61(2):292–3.

Crowley LC, Chojnowski G, Waterhouse NJ. Measuring the DNA content of cells in apoptosis and at different cell-cycle stages by propidium iodide staining and flow cytometry. Cold Spring Harb Protoc, 2016a; 2016(10).

Crowley LC, Marfell BJ, Scott AP, Waterhouse NJ. Quantitation of apoptosis and necrosis by annexin V binding, propidium iodide uptake, and flow cytometry. Cold Spring Harb Protoc, 2016b; 2016(11).

El-Hawary SS, Mohammed R, Tawfike AF, Lithy NM, AbouZid SF, Amin MN, et al. Cytotoxic activity and metabolic profiling of fifteen *Euphorbia* species. Metabolites, 2020; 11(1).

El-Manawaty M, Fayad W, El-Fiky N, Wassel G, El-Menshawi B. High-throughput screening of 75 euphorbiaceae and myrtaceae plant extracts for in-vitro antitumor and pro-apoptotic activities on human tumor cell lines, and lethality to brine shrimp. Int J Pharm Pharm Sci, 2013; 5:178–83.

Evan GI, Vousden KH. Proliferation, cell cycle and apoptosis in cancer. Nature, 2001; 411(6835):342–8.

Farozi A, Banday JA, Shah SA. Genicunolide A, B and C: Three new triterpenoids from *Euphorbia geniculata*. Beilstein J Org Chem, 2015; 11:2707–12.

Ghante MH, Jamkhande PG. Role of pentacyclic triterpenoids in chemoprevention and anticancer treatment: an overview on targets and underling mechanisms. J Pharmacopunct, 2019; 22(2):55–67.

Govindachari TR, Viswanathan N, Pai BR, Rao R, Srinivasan M. Triterpenes of *Calophyllum inophyllum* Linn. Tetrahedron, 1967; 23(4):1901–10.

Holohan C, Van Schaeybroeck S, Longley DB, Johnston PG. Cancer drug resistance: an evolving paradigm. Nat Rev Cancer, 2013; 13(10):714–26.

Housman G, Byler S, Heerboth S, Lapinska K, Longacre M, Snyder N, et al. Drug resistance in cancer: an overview. Cancers, 2014; 6(3):1769–92.

Jamal A, Yaacob W, Din LB. Triterpenes from the root bark of *Phyllanthus Columnaris*. Aust J Basic Appl Sci, 2009; 3:1428–31.

Koay Y, Wong K, Osman H, Eldeen IMs, Asmawi M. Chemical Constituents and Biological Activities of *Strobilanthes crispus* L. Rec Nat Prod, 2013; 7:59–64.

Kumar P, Nagarajan A, Uchil PD. Analysis of cell viability by the MTT assay. Cold Spring Harb Protoc, 2018; 2018(6).

Martucciello S, Balestrieri ML, Felice F, Estevam Cdos S, Sant'Ana AE, Pizza C, et al. Effects of triterpene derivatives from *Maytenus rigida* on VEGF-induced Kaposi's sarcoma cell proliferation. Chem Biol Interact, 2010; 183(3):450–4.

Min Z-d, Mizuo M, Toshiyuki T, Munekazu I, Xu G-Y, Huang Q-J. A diterpene from *Euphorbia antiquorum*. Phytochemistry, 1989; 28:553–5.

Monkodkaew S, Loetchutinat C, Nuntasaen N, Pompimon W. Identification and antiproliferative activity evaluation of a series of triterpenoids isolated from *Flueggea virosa* (Roxb. ex Willd.). Am J Appl Sci, 2009; 6(10):1800–6.

Ndwigah SN, Thoithi GN, Mwangi JW, Amugune BK, Mugo HN, Kibwage IO. Phytosterols from *Dombeya torrida* (J. F. Gmel.) East Cent Afr J Pharm Sci, 2013; 16:44–8.

Oliveira JPC, Ferreira ELF, Chaves MH, Militão GCG, Gerardo MV, Costa AM, Pessoa C, de Moraes MO, Costa-Lotufo LV. Chemical constituents of *Lecythis pisonis* and cytotoxic activity. Rev Bras Farmacogn, 2012; 22(5):1140–4.

Perumal PC, Sowmya S, Velmurugan D, Sivaraman T, Gopalakrishnan VK. Assessment of dual inhibitory activity of epifriedelanol isolated from *Cayratia trifolia* against ovarian cancer. Bangladesh J Pharmacol, 2016; 11(2):545–51.

Pistritto G, Trisciuoglio D, Ceci C, Garufi A, D'Orazi G. Apoptosis as anticancer mechanism: function and dysfunction of its modulators and targeted therapeutic strategies. Aging, 2016; 8(4):603–19.

Shi Q-W, Su X-H, Kiyota H. Chemical and pharmacological research of the plants in genus *Euphorbia*. Chem Rev, 2008;108(10): 4295–327.

Su M, Wu X, Chung HY, Li Y, Ye W. Antiproliferative activities of five Chinese medicinal herbs and active compounds in *Elephantopus scaber*. Nat Prod Commun, 2009; 4(8):1025–30.

Sun Y, Liu Y, Ma X, Hu H. The influence of cell cycle regulation on chemotherapy. Int J Mol Sci, 2021; 22(13):6923.

Wilaputraka IGNRB, Azminah A, Erlina L, Syahdi RR, Yanuar A. Virtual screening of indonesian herbal database for dna methyltransferase inhibitors. Asian J Pharm Clin Res, 2017; 10(Special Issue October):153–7.

Wong RS. Apoptosis in cancer: from pathogenesis to treatment. J Exp Clin Cancer Res, 2011; 30(1):87.

Wongprayoon P, Charoensuksai P. Cytotoxic and anti-migratory activities from hydroalcoholic extract of *Euphorbia lactea* Haw. against HN22 cell line. Thai Bull Pharm Sci, 2018; 13(1):69–77.Wongrakpanich A, Charoensuksai P. Induction of apoptosis in cancer cells by plants in the genus euphorbia. Thai Bull Pharm Sci, 2018; 13(2):1–11.

Yessoufou K, Elansary HO, Mahmoud EA, Skalicka-Woźniak K. Antifungal, antibacterial and anticancer activities of *Ficus drupacea* L. stem bark extract and biologically active isolated compounds. Ind Crops Prod, 2015; 74:752–8.

How to cite this article:
Wongprayoon P, Leelasart S, Jantham J, Pootaeng-on Y, Oekchuae S, Limpachayaporn P, Rayanil K, Charoensuksai P. A triterpenoid friedelan-3β-ol isolated from *Euphorbia lactea* exhibited cytotoxic activity against HN22 cells by inducing an S-phase cell cycle arrest. J Appl Pharm Sci, 2022; 12(10):031–048.

SUPPLEMENTARY MATERIAL

The online version of this article contains Supplementary Materials: ^{1}H-NMR, ^{13}C-NMR, and HRESIMS spectra of **1**–**4**.

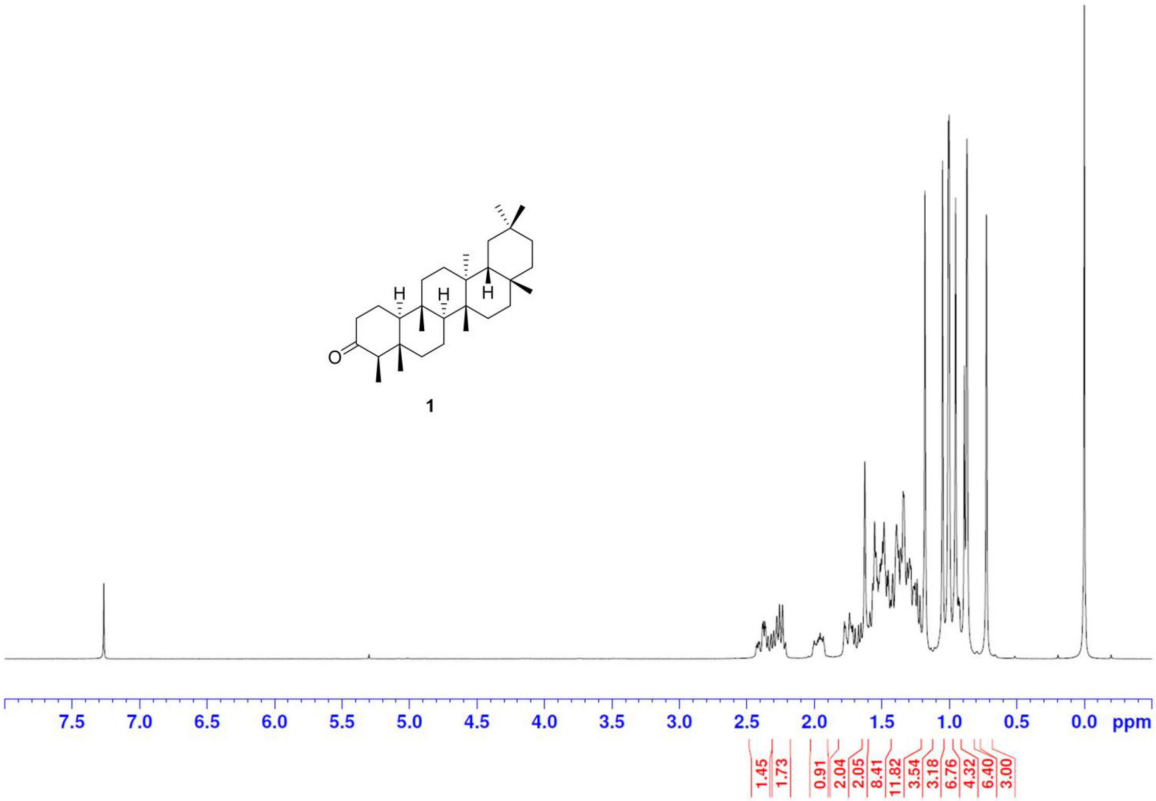

S1. ^{1}H NMR spectrum of **1** (300 MHz, $CDCl_3$)

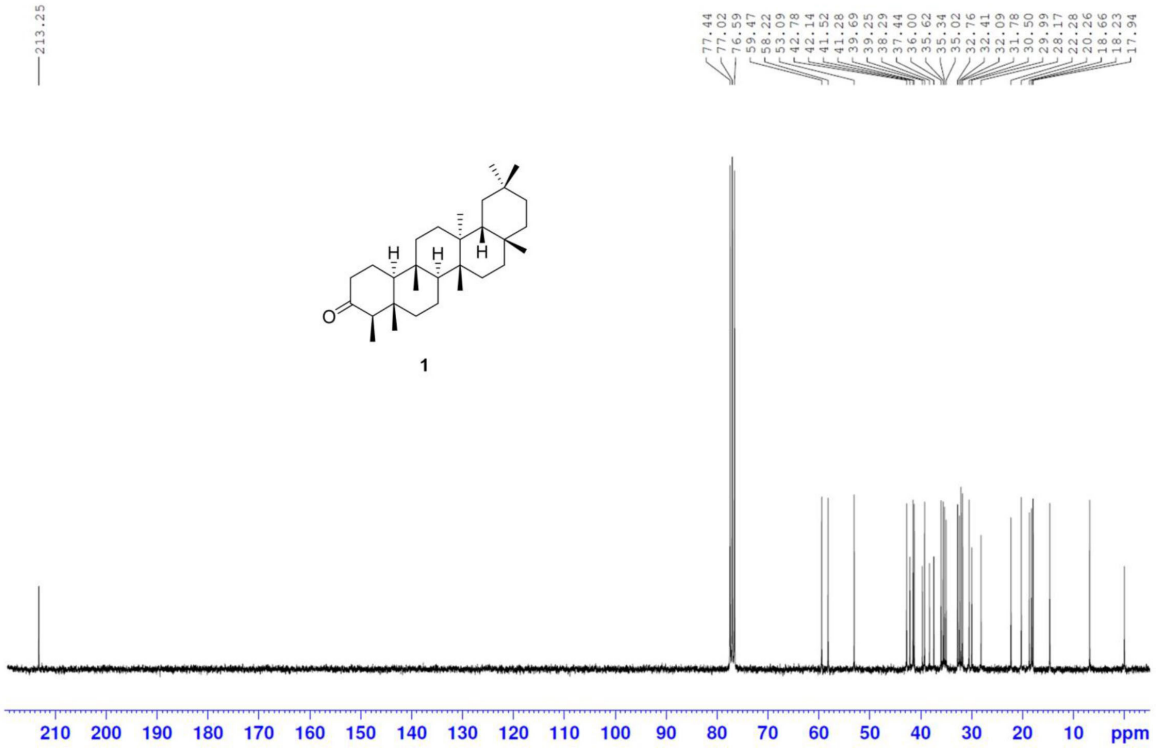

S2. ^{13}C NMR spectrum of **1** (75 MHz, $CDCl_3$)

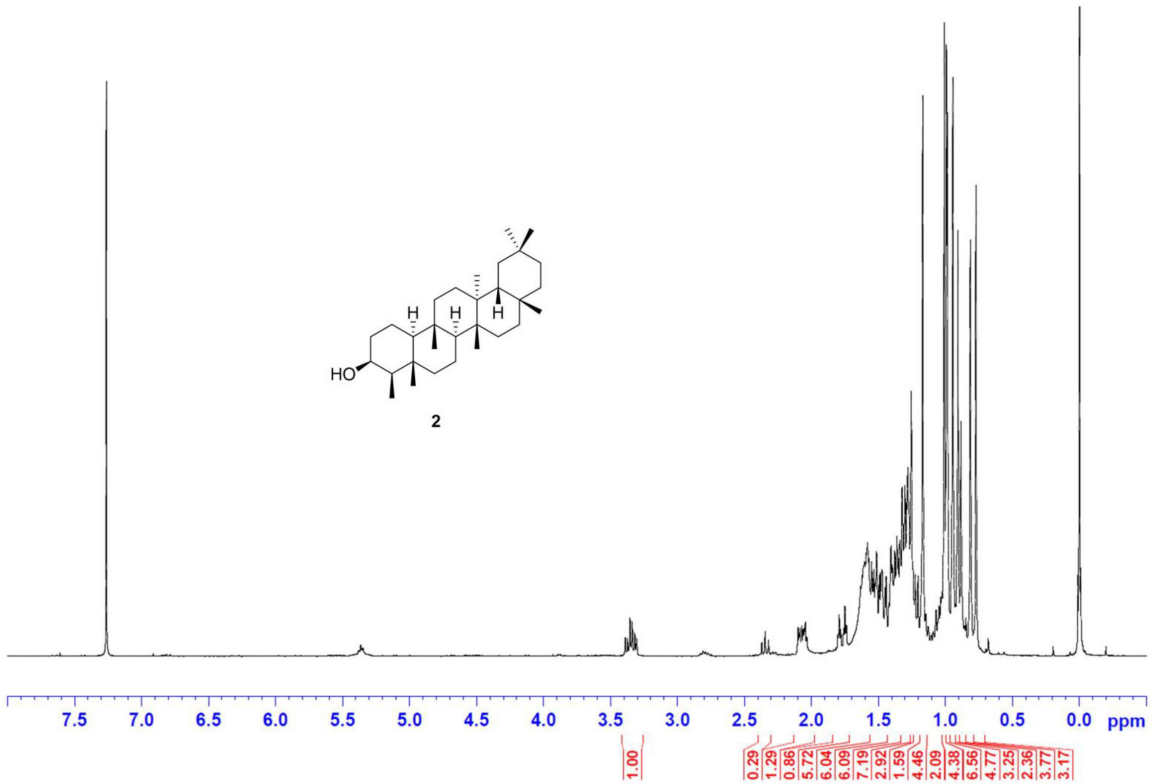

S3. ^{1}H NMR spectrum of **2** (300 MHz, $CDCl_3$)

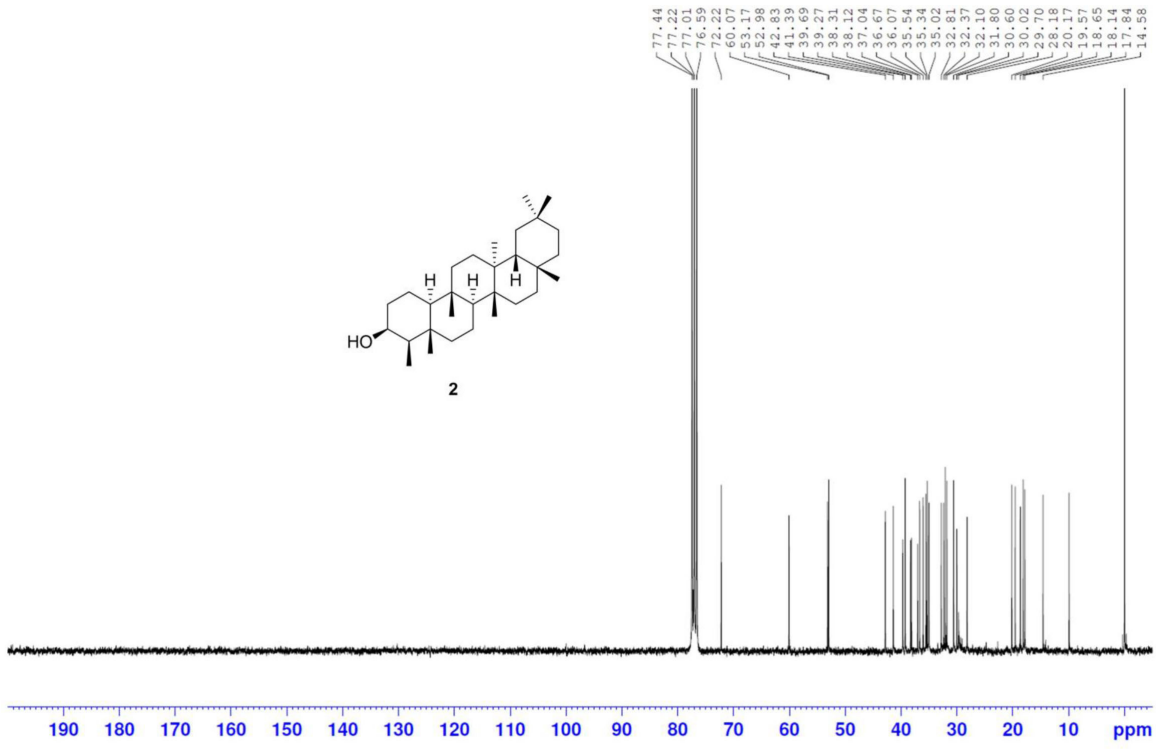

S4. ^{13}C NMR spectrum of **2** (75 MHz, $CDCl_3$)

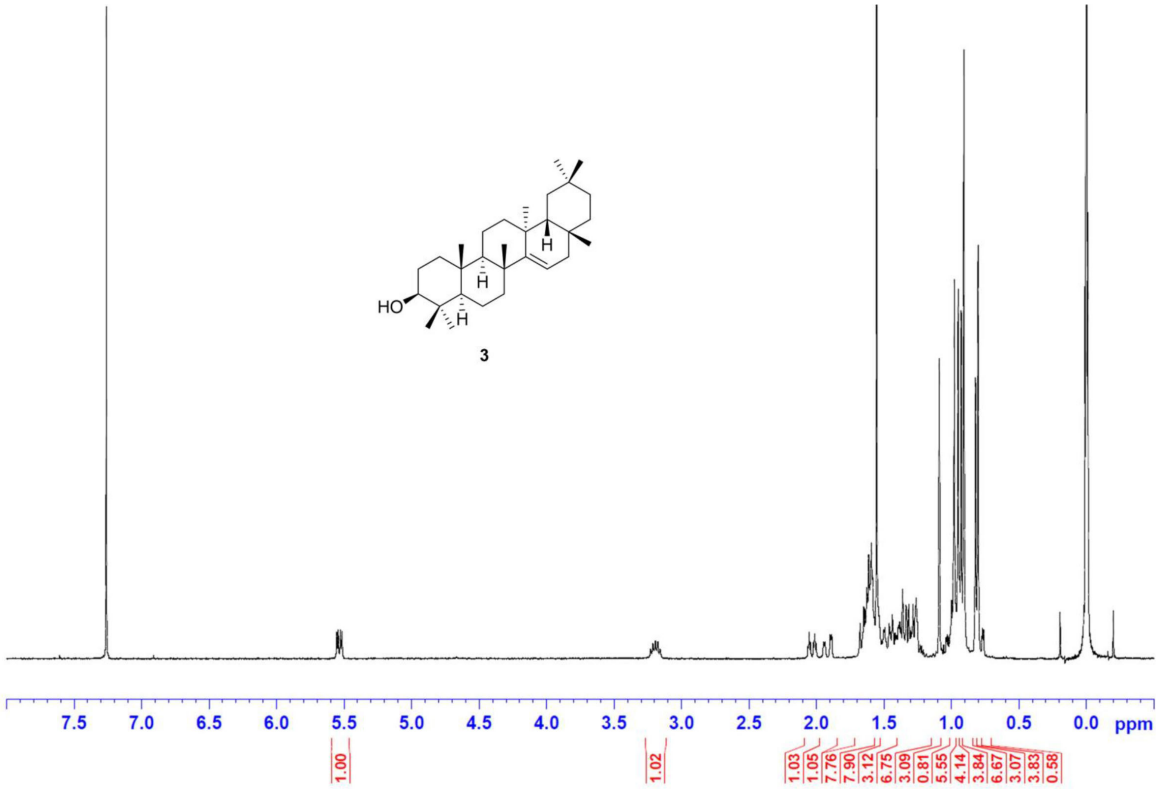

S5. ^{1}H NMR spectrum of **3** (300 MHz, $CDCl_3$)

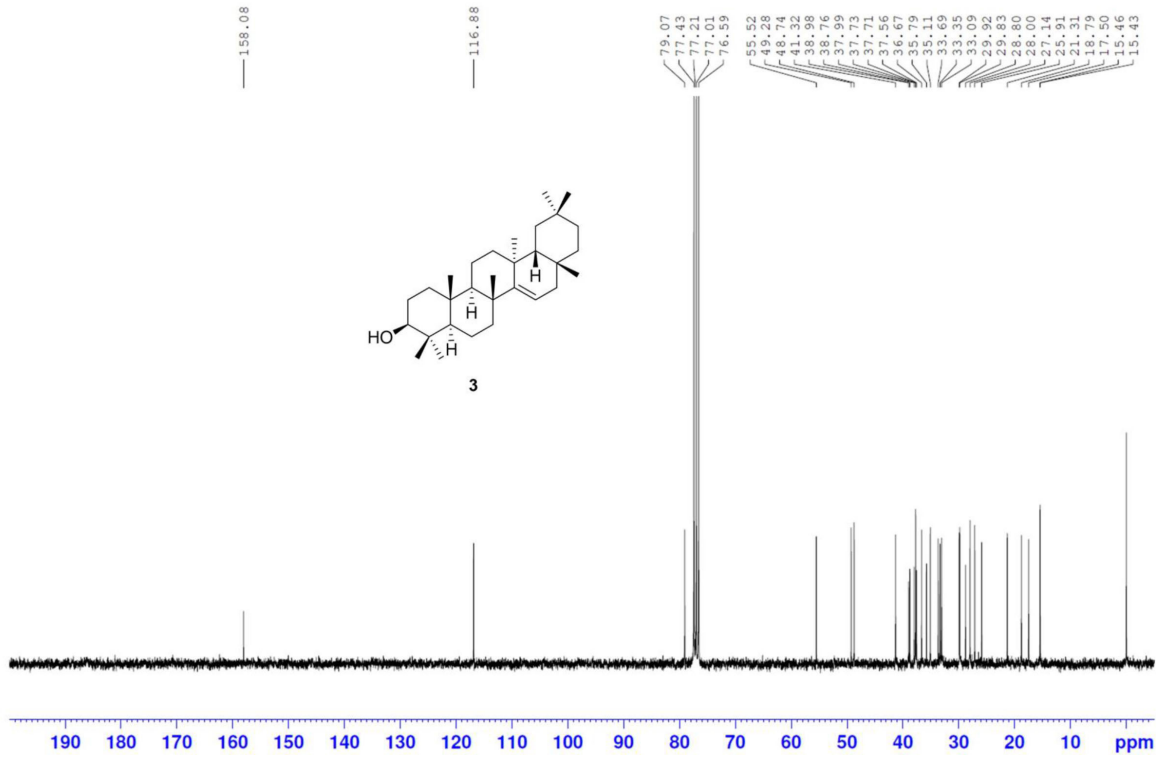

S6. ^{13}C NMR spectrum of **3** (75 MHz, $CDCl_3$)

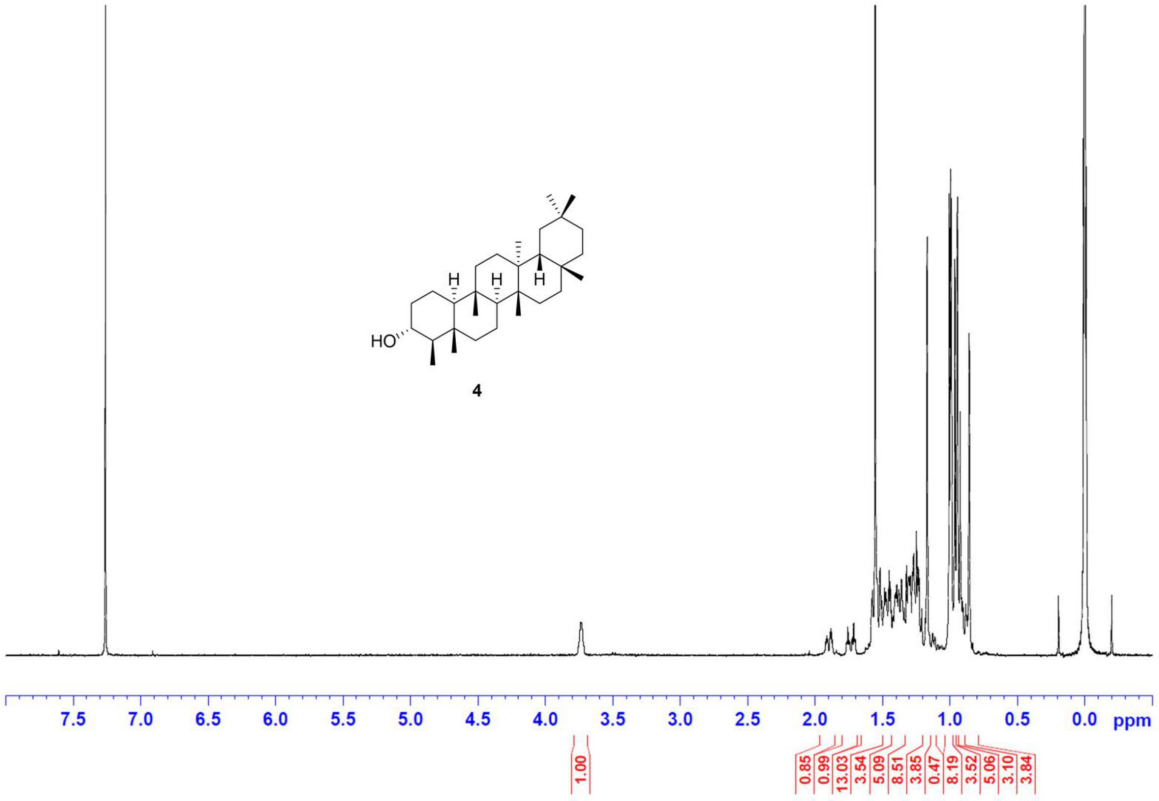

S7. ^{1}H NMR spectrum of **4** (300 MHz, $CDCl_3$)

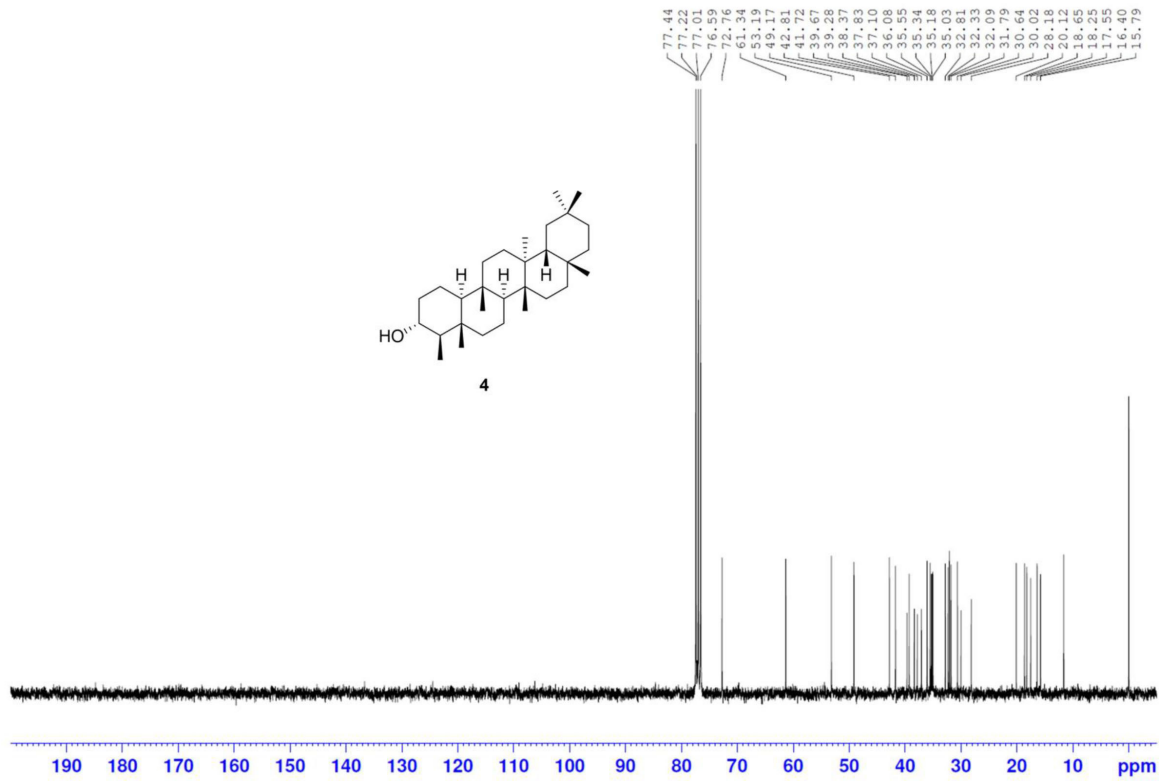

S8. ^{13}C NMR spectrum of **4** (75 MHz, $CDCl_3$)

Mass Spectrum List Report

Analysis Info

Analysis Name	OSSSUJJ12112019001_1.d	Acquisition Date	11/12/2019 9:13:26 AM
Method	Tune_low_1_POS_2019.m	Operator	Administrator
Sample Name	EL-1	Instrument	micrOTOF 72
	EL-1		

Acquisition Parameter

Source Type	ESI	Ion Polarity	Positive	Set Corrector Fill	50 V
Scan Range	n/a	Capillary Exit	150.0 V	Set Pulsar Pull	337 V
Scan Begin	50 m/z	Hexapole RF	150.0 V	Set Pulsar Push	337 V
Scan End	3000 m/z	Skimmer 1	45.0 V	Set Reflector	1300 V
		Hexapole 1	24.3 V	Set Flight Tube	9000 V
				Set Detector TOF	2295 V

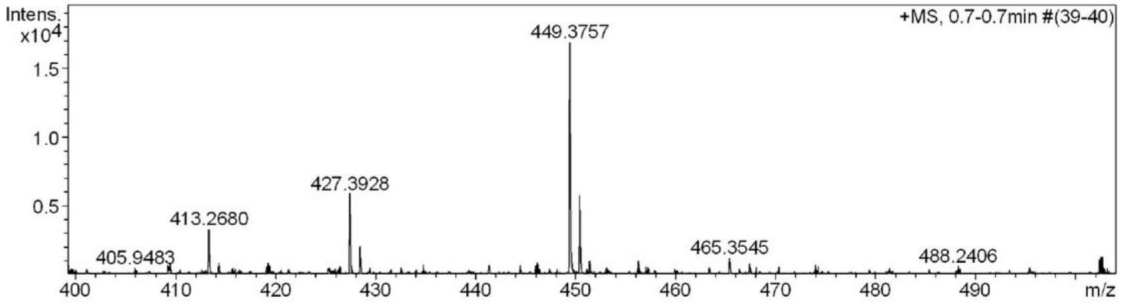

#	m/z	I	I %	S/N	Res.
1	401.1250	395	2.3	3.6	4786
2	405.9483	443	2.6	4.6	25242
3	410.3854	318	1.9	3.3	7094
4	413.2680	3221	19.1	33.5	4788
5	414.2696	799	4.7	8.3	4350
6	415.6565	422	2.5	4.4	23762
7	421.2443	318	1.9	3.3	3642
8	425.3613	449	2.7	4.7	4542
9	426.3521	528	3.1	5.5	21620
10	427.3928	5857	34.8	61.5	4973
11	428.3989	2034	12.1	21.4	4718
12	434.7231	677	4.0	7.1	33654
13	441.3040	638	3.8	6.8	3960
14	444.4214	613	3.6	6.5	5726
15	447.3517	329	2.0	3.5	4361
16	448.1120	327	1.9	3.5	30983
17	449.3757	16824	100.0	178.9	4915
18	450.3776	5712	34.0	60.8	4886
19	451.3809	964	5.7	10.3	3828
20	453.0642	452	2.7	4.8	17765
21	456.2318	951	5.7	10.2	27841
22	456.9782	538	3.2	5.8	33078
23	459.9102	370	2.2	4.0	32464
24	463.3489	469	2.8	5.0	4639
25	465.3545	1161	6.9	12.5	4265
26	467.3793	709	4.2	7.6	3547
27	473.9528	676	4.0	7.3	30333
28	479.3758	310	1.8	3.4	4332
29	488.2406	556	3.3	6.0	19943
30	502.4428	1247	7.4	13.7	22397

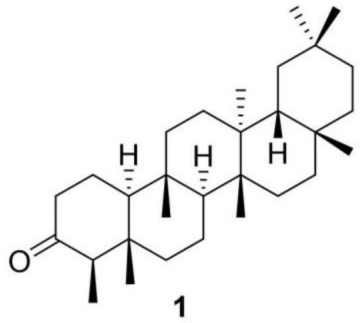

1

Chemical Formula: $C_{30}H_{50}O$

Exact Mass: 426.3862

HRMS m/z $[M+Na]^+$ 449.3757

calcd. for $C_{30}H_{50}ONa$ 449.3760

S9. HRESIMS spectrum of **1**

Mass Spectrum List Report

Analysis Info

Analysis Name	OSSSUJJ12112019002.d	Acquisition Date	11/12/2019 9:16:21 AM
Method	Tune_low_1_POS_2019.m	Operator	Administrator
Sample Name	EL-2 EL-2	Instrument	micrOTOF 72

Acquisition Parameter

Source Type	ESI	Ion Polarity	Positive	Set Corrector Fill	50 V
Scan Range	n/a	Capillary Exit	180.0 V	Set Pulsar Pull	337 V
Scan Begin	50 m/z	Hexapole RF	150.0 V	Set Pulsar Push	337 V
Scan End	3000 m/z	Skimmer 1	45.0 V	Set Reflector	1300 V
		Hexapole 1	24.3 V	Set Flight Tube	9000 V
				Set Detector TOF	2295 V

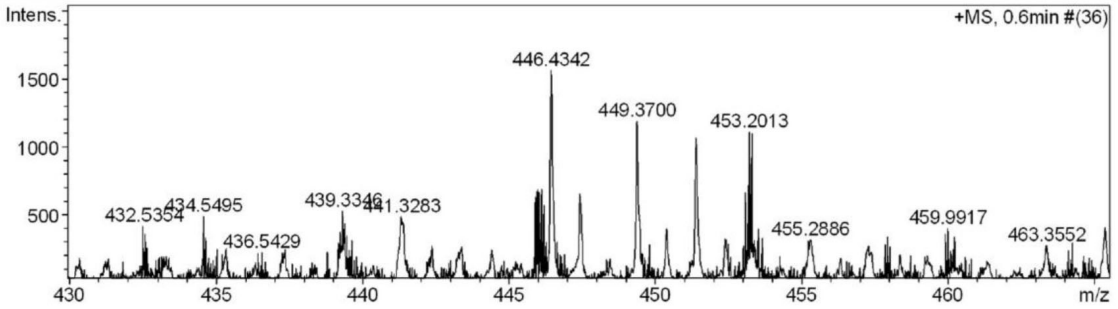

#	m/z	I	I %	S/N	Res.
1	431.3152	124	8.2	1.3	6563
2	432.5354	178	11.8	1.9	23030
3	433.2503	109	7.2	1.2	4903
4	434.3637	101	6.7	0.5	5513
5	434.5495	438	29.0	4.7	28043
6	436.5429	174	11.5	1.9	35069
7	437.3111	161	10.7	1.7	3289
8	438.2535	98	6.5	1.1	26400
9	439.3346	229	15.2	2.5	5652
10	441.3283	390	25.8	4.2	33165
11	442.3512	218	14.5	2.4	5978
12	443.3407	191	12.7	2.1	3187
13	444.4053	190	12.6	2.1	4021
14	446.4342	1507	100.0	16.4	5103
15	447.4270	574	38.1	6.2	4108
16	448.3323	118	7.9	1.3	24830
17	449.3700	1137	75.4	12.4	5551
18	450.3782	343	22.8	3.7	5655
19	451.3859	1014	67.3	11.0	4582
20	452.3890	264	17.5	2.9	3834
21	453.2013	1055	70.0	11.5	24459
22	455.2886	263	17.5	2.9	3520
23	456.3153	130	8.6	1.4	5638
24	457.2503	196	13.0	2.1	2143
25	457.9343	285	18.9	3.1	33666
26	458.3546	151	10.0	1.7	7205
27	459.2838	147	9.8	1.6	3506
28	459.9917	348	23.1	3.8	24166
29	460.2056	285	18.9	3.1	20133
30	463.3552	223	14.8	2.4	3804

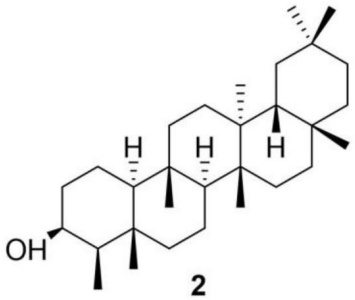

2

Chemical Formula: $C_{30}H_{52}O$

Exact Mass: 428.4018

HRMS m/z $[M+NH_4]^+$ 446.4342

calcd. for $C_{30}H_{52}O+NH_4$ 446.4356

S10. HRESIMS spectrum of **2**

Mass Spectrum List Report

Analysis Info

Analysis Name	OSSSUJJ12112019002.d	Acquisition Date	11/12/2019 9:16:21 AM
Method	Tune_low_1_POS_2019.m	Operator	Administrator
Sample Name	EL-2	Instrument	micrOTOF 72
	EL-2		

Acquisition Parameter

Source Type	ESI	Ion Polarity	Positive	Set Corrector Fill	50 V
Scan Range	n/a	Capillary Exit	180.0 V	Set Pulsar Pull	337 V
Scan Begin	50 m/z	Hexapole RF	150.0 V	Set Pulsar Push	337 V
Scan End	3000 m/z	Skimmer 1	45.0 V	Set Reflector	1300 V
		Hexapole 1	24.3 V	Set Flight Tube	9000 V
				Set Detector TOF	2295 V

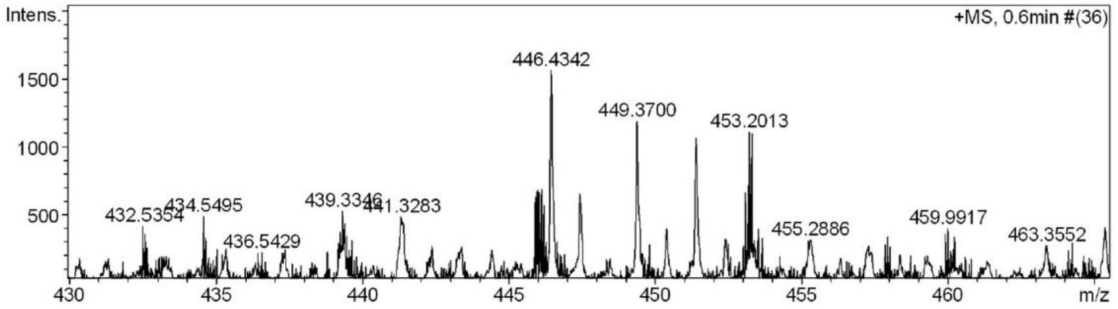

#	m/z	I	I %	S/N	Res.
1	431.3152	124	8.2	1.3	6563
2	432.5354	178	11.8	1.9	23030
3	433.2503	109	7.2	1.2	4903
4	434.3637	101	6.7	0.5	5513
5	434.5495	438	29.0	4.7	28043
6	436.5429	174	11.5	1.9	35069
7	437.3111	161	10.7	1.7	3289
8	438.2535	98	6.5	1.1	26400
9	439.3346	229	15.2	2.5	5652
10	441.3283	390	25.8	4.2	33165
11	442.3512	218	14.5	2.4	5978
12	443.3407	191	12.7	2.1	3187
13	444.4053	190	12.6	2.1	4021
14	446.4342	1507	100.0	16.4	5103
15	447.4270	574	38.1	6.2	4108
16	448.3323	118	7.9	1.3	24830
17	449.3700	1137	75.4	12.4	5551
18	450.3782	343	22.8	3.7	5655
19	451.3859	1014	67.3	11.0	4582
20	452.3890	264	17.5	2.9	3834
21	453.2013	1055	70.0	11.5	24459
22	455.2886	263	17.5	2.9	3520
23	456.3153	130	8.6	1.4	5638
24	457.2503	196	13.0	2.1	2143
25	457.9343	285	18.9	3.1	33666
26	458.3546	151	10.0	1.7	7205
27	459.2838	147	9.8	1.6	3506
28	459.9917	348	23.1	3.8	24166
29	460.2056	285	18.9	3.1	20133
30	463.3552	223	14.8	2.4	3804

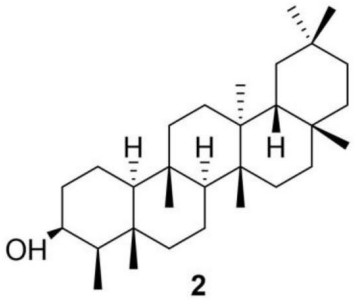

2

Chemical Formula: $C_{30}H_{52}O$

Exact Mass: 428.4018

HRMS m/z $[M+NH_4]^+$ 446.4342

calcd. for $C_{30}H_{52}O+NH_4$ 446.4356

S11. HRESIMS spectrum of **3**

Mass Spectrum List Report

Analysis Info

Analysis Name	OSSSUJJ12112019004.d	Acquisition Date	11/12/2019 9:25:04 AM
Method	Tune_low_1_POS_2019.m	Operator	Administrator
Sample Name	EL-4	Instrument	micrOTOF 72
	EL-4		

Acquisition Parameter

Source Type	ESI	Ion Polarity	Positive	Set Corrector Fill	50 V
Scan Range	n/a	Capillary Exit	130.0 V	Set Pulsar Pull	337 V
Scan Begin	50 m/z	Hexapole RF	150.0 V	Set Pulsar Push	337 V
Scan End	3000 m/z	Skimmer 1	45.0 V	Set Reflector	1300 V
		Hexapole 1	24.3 V	Set Flight Tube	9000 V
				Set Detector TOF	2295 V

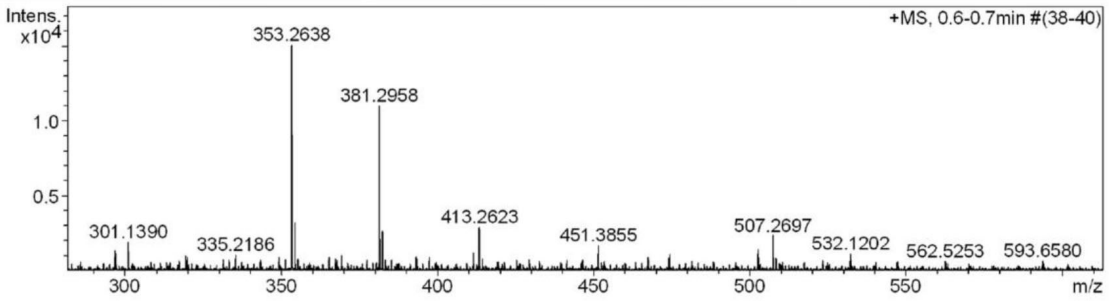

#	m/z	I	I %	S/N	Res.
1	56.2887	1668	11.1	18.1	5154
2	66.4298	1536	10.2	16.7	9869
3	89.2626	1669	11.1	18.1	11677
4	115.4597	1532	10.2	16.6	12441
5	129.8178	1685	11.2	18.3	5923
6	144.9884	1456	9.7	15.8	12202
7	145.0132	1602	10.6	17.4	12321
8	195.6394	1370	9.1	14.5	20721
9	296.9208	1370	9.1	13.8	17666
10	301.1390	1904	12.6	19.4	4643
11	353.2638	15077	100.0	155.9	4633
12	354.2673	3201	21.2	32.7	4705
13	381.2958	10989	72.9	115.7	4725
14	382.3005	2579	17.1	26.8	4607
15	413.2623	2888	19.2	30.7	4540
16	451.3855	1699	11.3	18.3	4614
17	502.6695	1429	9.5	15.9	27148
18	507.2697	2321	15.4	26.3	4148
19	711.5705	1543	10.2	18.1	4597
20	1075.7455	1565	10.4	19.7	33631
21	1443.0594	1707	11.3	25.4	45160
22	1864.2316	1533	10.2	22.7	54504
23	2339.1501	2040	13.5	33.0	70594
24	2339.2632	2463	16.3	39.9	72941
25	2339.3274	1701	11.3	27.4	28028
26	2596.9773	1408	9.3	23.0	65903
27	2868.0472	1529	10.1	24.5	73314
28	2868.1580	1628	10.8	26.1	58562
29	2868.3972	2018	13.4	32.4	72710
30	2868.5968	1330	8.8	21.2	49586

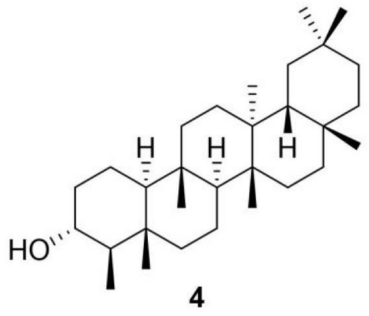

4

Chemical Formula: $C_{30}H_{52}O$
Exact Mass: 428.4018
HRMS m/z $[M+Na]^+$ 451.3855
calcd. for $C_{30}H_{52}ONa$ 451.3916

S12. HRESIMS spectrum of **4**